



# Probabilistic Stress Intensity Factor Prediction of Surface Crack Using Bootstrap Sampling Method

M.N.M. Husnain<sup>1</sup>, M.R.M. Akramin<sup>1\*</sup>, Z.L. Chuan<sup>2</sup>, M.S. Shaari<sup>1</sup>, Akiyuki Takahashi<sup>3</sup>, M.H. Akmal<sup>1</sup>

<sup>1</sup>Faculty of Mechanical & Automotive Engineering Technology,  
Universiti Malaysia Pahang, 26600 Pekan, Pahang Darul Makmur, MALAYSIA

<sup>2</sup>Faculty of Industrial Sciences & Technology,  
Universiti Malaysia Pahang, Lebuhraya Tun Razak, 26300 Gambang, Kuantan Pahang Darul Makmur, MALAYSIA

<sup>3</sup>Faculty of Science and Technology, Department of Mechanical Engineering,  
Tokyo University of Science, 2641 Yamazaki, Noda, Chiba 278-8510, JAPAN

\*Corresponding Author

DOI: <https://doi.org/10.30880/ijie.2022.14.08.015>

Received 30 May 2022; Accepted 28 November 2022; Available online 21 December 2022

**Abstract:** Fatigue cracks commonly occur for in-service engineering structures. The main parameter for fatigue crack is the stress intensity factor (SIF). The SIF is an indicator of the fatigue crack growth and remaining life of a structure. Nonetheless, a problem was raised when determining the remaining life since the SIF could not be presented in physical phenomena. Thus, a technique is required to predict the range of SIF. Maximum and minimum bounds of SIF help estimate the range of remaining life. This paper aims to predict a structure's safe and failure region during the fracture process based on the SIFs. The primary tool is S-version Finite Element Model (S-FEM). Yet, S-FEM unable to compute random variables in analysis. Thus, the Bootstrap is developed and embedded into S-FEM for computing random variables in the analysis. The random variables are utilised to predict a range of SIFs. The SIFs are generated based on one hundred samples. The samples are randomly generated based on the distribution of material properties. A lognormal distribution is used to generate the material properties. The sampling process is computed based on the bootstrap method. The embedded Bootstrap in S-FEM was introduced as BootstrapS-FEM. When the samples exceed the fracture toughness of 29 MPa $\sqrt{m}$ , the failure region is indicated at the angle  $2\phi/\pi = 0.627$  to 1 with 6% of failure samples. The safe region is observed at angle  $2\phi/\pi = 0$  to 0.626 with 94% of the samples. The failure region is essential in this analysis to prevent unstable crack growth.

**Keywords:** Fatigue cracks, stress intensity factor, s-fem, finite element method

## 1. Introduction

Many factors contribute to the crack growth rate, including the flaw's size [1], shape, orientation [2] and location. The factors of crack growth rate occur in a scatter presented in actual data. The scatter results produce variations in the crack growth parameters such as material properties and crack size. The material properties mainly influence the fatigue parameters; hence, SIF and fatigue behaviour variations will be generated automatically. The randomness in some of the parameters reveals the complexity of the analysis of the surface cracks. The calculation of SIF for surface cracks significantly influenced the lifetime of the material structures.

\*Corresponding author: [akramin@ump.edu.my](mailto:akramin@ump.edu.my)

2022 UTHM Publisher. All rights reserved.

[penerbit.uthm.edu.my/ojs/index.php/ijie](http://penerbit.uthm.edu.my/ojs/index.php/ijie)

The three-dimensional fatigue crack propagation analysis of surface cracks is gaining more attention from researchers. The SIF of three-dimensional fatigue crack propagation must be computed along the whole crack front. The SIF was too dependent on crack depth and crack aspect ratio [3]. Nonetheless, the crack depth and crack aspect ratio were exposed to the uncertainty in size [4]. Thus, SIF was unable to calculate precisely. Many researchers have introduced calculating SIF numerically [5], but it was limited to specific geometry only. For complex geometry, finite element method is the option. Since the SIF was calculated by computation for complex geometry, physical validation by experiment was unable to embark [6]. Thus, a range of SIF calculations is needed for better estimation of SIF which is exposed to the uncertainty in crack depth and crack aspect ratio [6].

Therefore, an analysis method is required which considers the uncertainties in the structural components of the application environment. One such method is the probabilistic analysis. In the probabilistic approach, the uncertainty can be considered with the upper and lower bounds. The bounds is computed from the sampling process [7]. The uncertain parameters are involved in the analysis, for instance loads, material properties and crack geometrical aspects.

The uncertainties considered in this analysis further ensure the safety of structures. Thus, the analysis of fatigue crack growth by probabilistic approach is adequate for predicting the detection period. The prediction is essential to ensure defects in the material components will not produce failure during the in-service schedule and the lifetime of the material composition can be estimated prior to the scheduled detection [8].

The probabilistic analysis estimates the output value of variables. It is dependent on the input data's uncertainty. Unlike deterministic analysis, deterministic analysis only produces a single output. In addition, the deterministic analysis produces output predefined by the input data set. The deterministic approach begins with single parameters, while the probabilistic approach begins with random parameters. Few probabilistic approaches are available such as Monte Carlo [9], Bootstrap [10] and many more. Thus, Bootstrap S-FEM was computed in this study.

Many applications implemented the Bootstrap method for fatigue assessment such as turbine blades [11], overload effects [12], pipelines [10], superalloy [13], fatigue lifetime [14] and many more. Bootstrap methods showed an excellent alternative for generating an abnormal distribution [15], reducing the time taken for the sampling process [12] and requiring fewer assumptions during the simulation process [16]. Thus, Bootstrap was embedded in S-FEM to integrate the uncertainties in the simulation process.

The FEM software was utilised to compute the SIFs. The three-dimensional of crack growth model is simulated using the Bootstrap and S-FEM. The advantage of S-FEM is to solve the re-meshing problem due to the complexity of a model. Thus, S-FEM is one of the solutions to simplify this problem. The SIF is simulated in a semi-elliptical surface crack shape using the S-FEM. Since determining SIF in fracture mechanics analysis is crucial, it is questionable for complex geometry. The numerical calculation is limited to the specific geometry only. FEM calculation was the solution but the SIF could not compare with the physical experiment. In addition, uncertainty in parameters ruined the accuracy of the SIF value.

Thus, this paper aims to calculate the SIF with a sampling technique such as Bootstrap method. The distribution of the sampling process for SIF is presented to determine the range of SIF value, safe region and failure region.

## 2. Methodology

The SIF was calculated based on the energy release rate on the crack opening. The energy release rate was converted to the SIF with certain parameters involved. This technique is called virtual crack closure-integral method, VCCM. Figure 1 presents the crack opening displacement,  $v_i$ . There are five critical nodes in each crack front's element. The nodes are represented as  $P_1$  until  $P_5$  in the VCCM. As well as, at the opening displacement,  $v_i$ , there are five critical nodes from  $v_1$  until  $v_5$ . The nodes are located at the edge of the crack front.

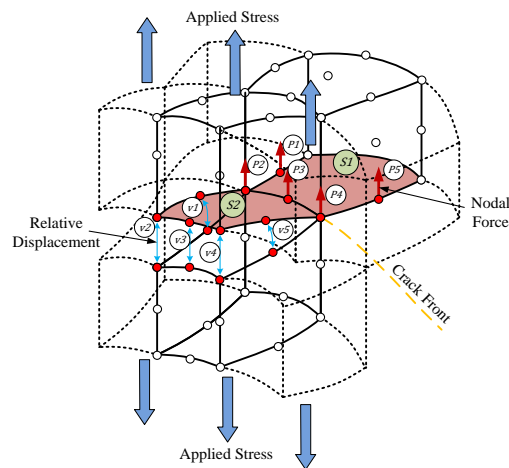


Fig. 1 - VCCM at the crack front

The opening displacement,  $v_i$  is determined based on the displacement from the lower,  $v_{iL}$  and upper  $v_{iU}$  surface crack.

$$v_i = v_{iU} - v_{iL} \tag{1}$$

Since there are global,  $G$  and local,  $L$  mesh, thus there are displacements for local and global for lower and upper surface crack. The displacement in global mesh for the lower surface crack is indicated as  $v_{iL}^G$ . Meanwhile, the upper surface crack in the local mesh is indicated as  $v_{iU}^L$ . The total displacement is summation of upper  $v_{iU}$  and lower  $v_{iL}$  surface cracks:

$$\begin{aligned} v_{iU} &= v_{iU}^G + v_{iU}^L \\ v_{iL} &= v_{iL}^G + v_{iL}^L \end{aligned} \tag{2}$$

In Bootstrap S-FEM, the crack growth only occurs in the local mesh; thus, the opening displacement in the global mesh remains zero. The updating mesh in the local region only is the main advantage of BootstrapS-FEM. It will reduce the computation time. Thus, the opening displacement,  $v_i$ , at the local mesh is expressed as

$$v_i = (v_{iU}^G + v_{iU}^L) - (v_{iL}^G + v_{iL}^L) = v_{iU}^L - v_{iL}^L \tag{3}$$

Once the opening displacement was calculated, the energy release rate could be determined. The calculation for energy release rate,  $G$  for the non-symmetrical at the crack front could be referred to by Okada et al. [17]-[19]. Based on Okada et al. technique, the energy spent,  $\Delta G_I$  could be calculated based on the area at the crack front. The area of the crack front is indicated as  $S_I$ . Therefore, the energy spent is expressed as

$$\Delta G_I = \frac{1}{2} \int_{S_1} \sigma_{33}(r) v_3(\Delta - r) dS \tag{4}$$

The  $\Delta$  length of the element and  $r$  is the width of the element. Figure 2 displays the top view of the element at the crack front. The  $\sigma_{33}$  is the cohesive stress. It is located at the plane of the crack front. The cohesive stress could be determined as

$$\sigma_{33}(\bar{r}) = \frac{K_I}{\sqrt{2\pi\bar{r}}}, \quad v_3(\bar{r}) = 4\sqrt{\frac{2\bar{r}}{\pi}} \frac{K_I}{E'} \tag{5}$$

where  $E$  and  $\nu$  represent the modulus elasticity and Poisson's ratio. Thus, substituting the stress and displacement into Eq. (3) gives

$$\Delta G_I = \int_{\theta_1}^{\theta_2} \int_0^{\Delta} \frac{K_I}{\sqrt{2\pi r \cos \varphi}} 2\sqrt{\frac{2(\Delta - r) \cos \varphi}{\pi}} \frac{K_I}{E'} (R + r) dr d\theta \tag{7}$$

Thus, Eq. (7) could be converted into the element areas of  $S_1$  and  $S_2$ . The element area is shown in Figure 2.

$$G_I = \frac{K_I^2}{E'} = \frac{1}{2 \left[ S_1 - \frac{1}{4}(S_1 - S_2) \right]} \sum_{i=1}^5 v_i^3 P_i^3 \tag{8}$$

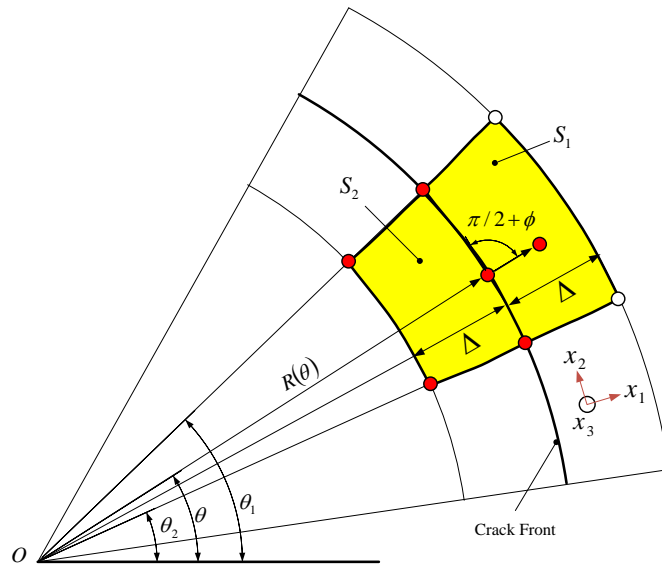


**Fig. 2 - Top view of the crack front's element**

The remaining energy release rate,  $G$  for different failure modes is computed based on

$$G_{II} = \frac{K_{II}^2}{E^1} = \frac{1}{2 \left[ S_1 - \frac{1}{4}(S_1 - S_2) \right]} \sum_{i=1}^5 v_i^1 P_i^1 \quad (9)$$

$$G_{III} = \frac{K_{III}^2}{2\mu} = \frac{1}{2 \left[ S_1 - \frac{1}{4}(S_1 - S_2) \right]} \sum_{i=1}^5 v_i^2 P_i^2 \quad (10)$$

The  $\mu$  is a shear modulus. There are three type of modes in fracture mechanics. For mode I, the energy release rate,  $G$ , is presented as  $G_I$ . The remaining modes II and III is presented as  $G_{II}$  and  $G_{III}$ , respectively. Thus, the energy release rate could convert into SIF as shown in Eq. (8), (9) and (10). This method was computed on a tension model. Figure 3 shows a tension model with a surface crack in the middle of the geometry. Fatigue load is applied at the top and bottom of the geometry.

The local stress and the crack depth relate to characterising the SIF. Experiments from the LFM concept also produce fracture toughness. Fracture toughness can oppose the material from fracture. If the value for SIF is greater than fracture toughness, then catastrophic failure will happen. Furthermore, the fracture process consists of three basic crack propagation modes based on the type of loadings. The three primary modes are; mode I (for tensile mode), mode II (for in-plane shear), and mode III (for anti-plane shear). All the modes could be combined to produce a mixed mode. For brittle materials, it had been examined to possess mode II and a mixed mode (mode I and mode II). The most important thing to note is that the mode for fatigue fracture not only describes the fatigue crack growth rate and analysis of crack paths. The SIF exists for other types of loading, but the most common mode I.

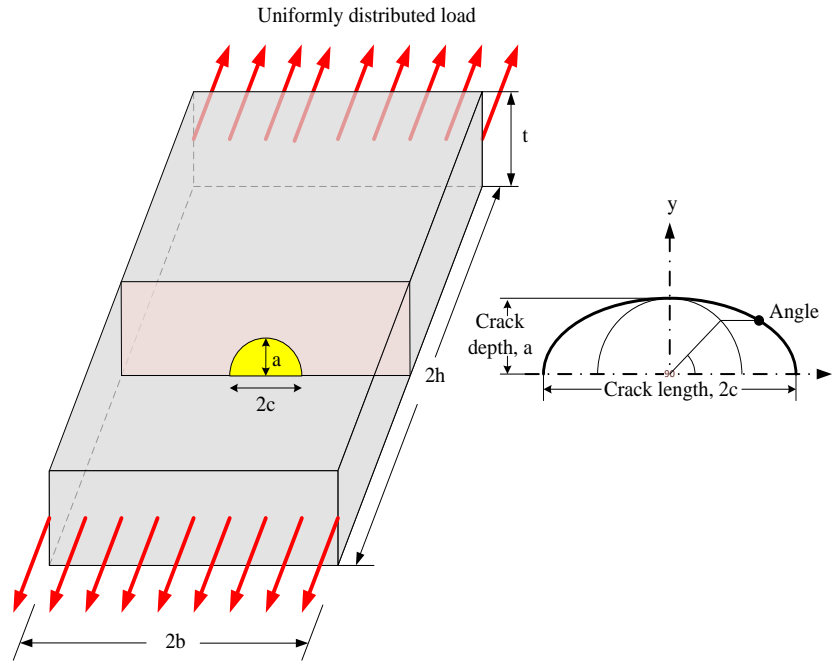


**Fig. 3 - Tension model for surface crack growth under tension load**

The proposed BootstrapS-FEM approach was conducted to simulate the SIFs in lognormal distributions. The constant amplitude loading was considered with 490 MPa. The load was less than the yield strength of the Aluminium Alloy 7075-T6, where it was considered as cracking in the fatigue region. The load used was also enough for elastic deformation based on the LEFM concept. Figure 4 shows the SIFs for a tension model along the crack front subjected to fatigue load. The crack aspect ratio was modelled with a mean 0.04 and standard deviation 0.01, then generated for one hundred samples using BootstrapS-FEM. The material properties for Aluminium Alloy 7075-T6 are shown in Table 1.

**Table 1 - Material properties of Aluminium Alloy 7075-T6**

Variables	Values
Fracture toughness, $K_{IC}$	29 MPa. $\sqrt{m}$
Young's modulus, $E$	71.7 GPa
Tensile strength, Yield	503 MPa
Poisson's ratio, $\nu$	0.33
Fatigue power parameter, $n$	2.88
Paris coefficient, $C$	$2.29 \times 10^{-10}$
The threshold value, $K_{th}$	5.66 MPa. $\sqrt{m}$

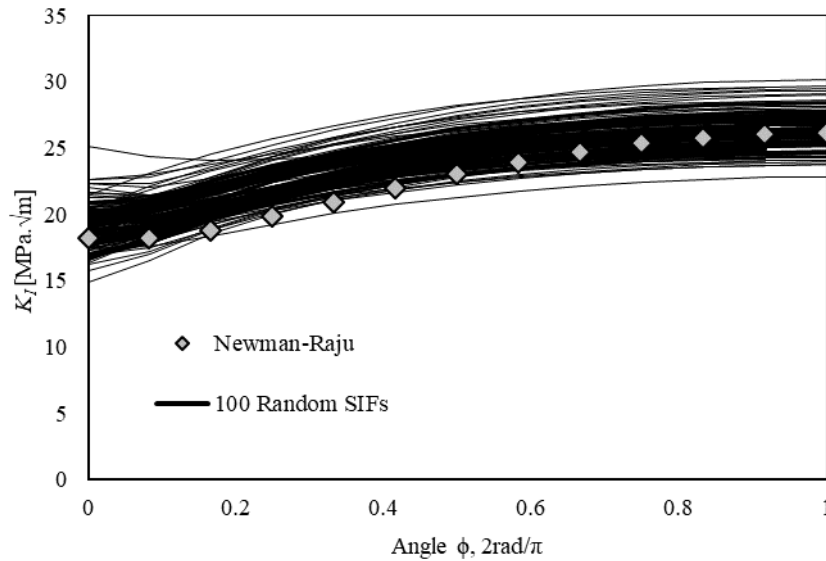
### 3. Result and Discussion

Figure 4 shows the generation of one hundred samples of SIFs under tension load. These random samples are generated using the BootstrapS-FEM. It shows all possibilities of SIFs value for the tension model from maximum to minimum value of SIF. If one angle was selected, the distribution of the SIF value could be computed such as in Figure 5. The angle is critical to show the higher propagation of the crack.

Figure 5 shows the comparison of SIF calculation by Newman-Raju and S-FEM. The Newman-Raju is calculated based on analytical solution. The S-FEM results show a good agreement with Newman-Raju. The deterministic S-FEM not reaching the fracture toughness of 29 MPa. $\sqrt{m}$  for Aluminium Alloy 7075-T6. During the fracture process, the safe structure was predicted below the critical SIF in the elastic region. Thus, the unstable crack growth did not occur based on the deterministic S-FEM approach because it only produced a single prediction of SIF. If one only relies on deterministic S-FEM, the fracture could occur because there is a possibility that the SIF might reach beyond critical SIF. Therefore, BootstrapS-FEM was utilised to predict the SIF value that possibly tends to achieve fracture toughness. The mean BootstrapS-FEM was presented with upper and lower bounds, as shown in Figure 5. The bounds were calculated using a 95% confidence level.

The upper bound exceeds the fracture toughness, thus indicating a significant probability for unstable crack growth. The failure region shown in the shaded area of Region A exceeds the fracture toughness from one part of the one hundred

samples at angle  $2\phi/\pi=0.627$  to 1, as depicted in Figure 5. Thus, a catastrophic failure of the material and the structural component could occur. Thus, the BootstrapS-FEM should be considered in the analysis since it is able to detect the possibility of unstable crack growth happening compared to deterministic S-FEM. Deterministic S-FEM produces passive results since a single graph was produced instead of a range of results on every crack angle.



**Fig. 4 - Samples of SIFs along the crack front**

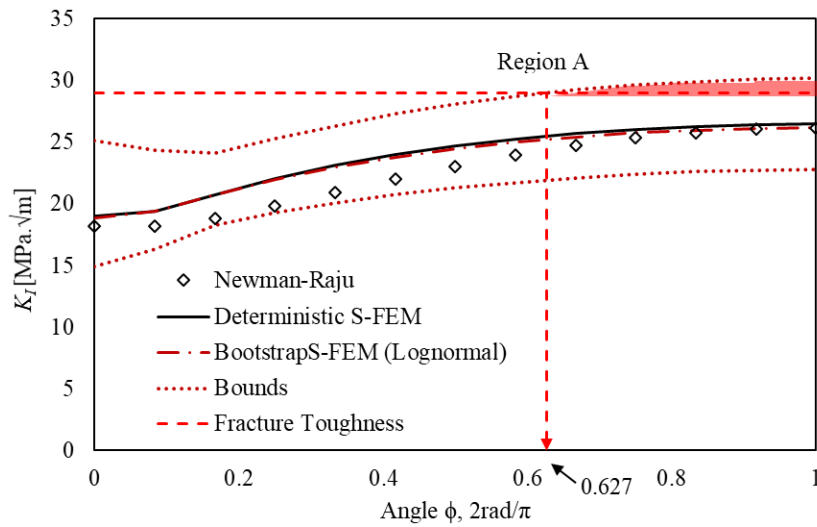


**Fig. 5 - The bounds of SIFs for tension model**

Figure 6 shows the histogram for the SIF at  $2\phi/\pi = 1$  for the tension model. The minimum and maximum stresses are 23.43 and 30.91 MPa·√m, respectively. The mean value is 27.35 MPa·√m. The minimum and maximum deviations from the mean are 3.92 and 3.56 MPa·√m, respectively. However, the minimum and maximum deviation ranges were only approximately 7.48 MPa·√m, it does not produce a significant uncertainty for generating one hundred samples. Even though it shows a small range of uncertainty, it is crucial when analysed with fracture toughness. In this case, the critical SIF was 29 MPa·√m. Thus, 94% of the samples were in the safe region, below the critical SIF. Catastrophic failure would not occur in the safe region. Figure 6 also shows the failure region with 6% of failure samples. The failure region means the occurrence of unstable crack growth. The unstable crack growth happens in material structures without warning. This prognosis cannot be generated by the deterministic method. The deterministic S-FEM approach predicts that the model is in a safe region at any angle. This result illustrates the cruciality of the probabilistic analysis in the framework of fatigue problems.

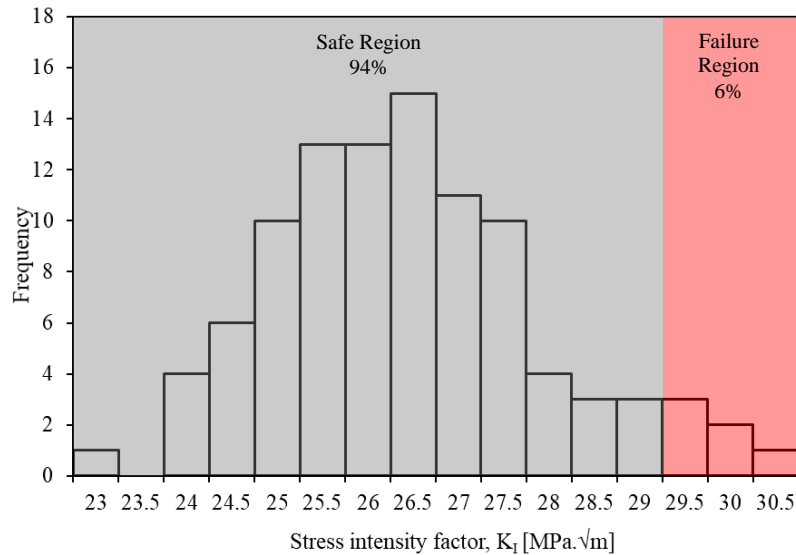


**Fig. 6 - Histogram of SIFs for safe and failure region in tension model**

#### 4. Conclusion

The probabilistic analysis helps prevent the material structure from failing. The prediction of BootstrapS-FEM and deterministic S-FEM is almost similar, but the BootstrapS-FEM could produce the lower and upper bounds of SIF. The bounds are crucial during decision-making since they produce a range of SIF values. The range of SIF will help in prioritising the maintenance proceeding. The probability of failure was 0.06 or 6%, which surpassed the fracture toughness. From the 100 generation samples of SIFs, the prediction of safe samples was 0.94 or 94%, which were further examined in safe mode to prevent unstable crack propagation. Thus, applying a bootstrap analysis in design is advisable in practical cases.

#### Acknowledgement

The author would like to acknowledge the Ministry of Higher Education under the Fundamental Research Grant Scheme FRGS/1/2019/TK03/UMP/02/21 (university reference RDU1901151) and Universiti Malaysia Pahang (UMP) for financial support.

#### References

- [1] Newman, J. C. (2015). Fatigue and Crack-growth Analyses under Giga-cycle Loading on Aluminum Alloys," *Procedia Engineering*, 101, 339-346.
- [2] Ciavarella, M., & Monno, F. (2006). On the possible generalizations of the Kitagawa-Takahashi diagram and of the El Haddad equation to finite life. *International Journal of Fatigue*, 28, 1826-1837.
- [3] Toribio, J., González, B., & Matos, J. C. (2022). Review and synthesis of stress intensity factor (SIF) solutions for circular inner cracks in round bars under tension loading. *Procedia Structural Integrity*, 37, 995-1000.
- [4] Georgsson, P. (2000) . The Determination of Uncertainties in Fatigue Crack Growth Measurement. Sweden: Volvo Aero Corporation.
- [5] Atroshchenko, E. (2010). Stress intensity factors for elliptical and semi-elliptical cracks subjected to an arbitrary mode I loading. Available: <http://libdspace.uwaterloo.ca/handle/10012/5166>.
- [6] Toribio, J., González, B., & Matos, J. C. (2021). Review and synthesis of stress intensity factor (SIF) solutions for elliptical surface cracks in round bars under tension loading: A tribute to Leonardo Torres-Quevedo. *Procedia Structural Integrity*, 37, 1029-1036.
- [7] Gao, W., Wu, D., Song, C., Tin-Loi, F., & Li, X. (2011). Hybrid probabilistic interval analysis of bar structures with uncertainty using a mixed perturbation Monte-Carlo method. *Finite Element in Analysis & Design*, 47, 643-652.
- [8] Gobbato, M., Conte, J. P., Kosmatka, J. B., & Farrar, C. R. (2012). A reliability-based framework for fatigue damage prognosis of composite aircraft structures," *Probabilistic Engineering Mechanics*, 29, 176-188.
- [9] Belyanna, M. A., Zeghida, C., Tlili, S., & Guedri, A., (2022). Piping reliability prediction using Monte Carlo simulation and artificial neural network. *Procedia Structural Integrity*, 41, 372-383.
- [10] Wang, X. (2022). Pipeline leakage alarm via bootstrap-based hypothesis testing. *Mechanical System & Signal Processing*, 179, 109334.
- [11] Abdallah, I., Tatsis, K., & Chatzi, E. (2017). Fatigue assessment of a wind turbine blade when output from

- multiple aero-elastic simulators are available. *Procedia Engineering*, 199, 3170-3175.
- [12] Jiang, S., & Zhang, W. (2022). A hybrid approach of modified bootstrap and physics-based methods for probabilistic fatigue life prediction considering overload effects. *Probabilistic Engineering Mechanics.*, 70, 103343.
- [13] Tan, L., Yang, X. G., Shi, D. Q., Hao, W. Q., & Fan, Y. S. (2022). Unified fatigue life modelling and uncertainty estimation of Ni-based superalloy family with a supervised machine learning approach. *Engineering Fracture Mechanics*, 275, 108813.
- [14] Bigerelle, M., Najjar, D., Fournier, B., Rupin, N., & Iost, A. (2005). Application of Lambda Distributions and Bootstrap analysis to the prediction of fatigue lifetime and confidence intervals. *International Journal of Fatigue*, 28, 223-236.
- [15] Moreno-Martínez, F. J., & Laws, K. R. (2007). An attenuation of the ‘normal’ category effect in patients with Alzheimer’s disease: A review and bootstrap analysis. *Brain & Cognition*, 63, 167-173.
- [16] Li, D. Q., Tang, X. S., & Phoon, K. K. (2015). Bootstrap method for characterizing the effect of uncertainty in shear strength parameters on slope reliability. *Reliability Engineering & System Safety*, 140, 99-106.
- [17] Okada, H., Kawai, H., & Araki, K. (2008). A virtual crack closure-integral method (VCCM) to compute the energy release rates and stress intensity factors based on quadratic tetrahedral finite elements,” *Engineering Fracture Mechanics*, 75, 4466-4485.
- [18] Okada, H., Higashi, M., Kikuchi, M, Fukui, Y., & Kumazawa, N. (2004). Three dimensional virtual crack closure-integral method (VCCM) with skewed and non-symmetric mesh arrangement at the crack front. *Engineering Fracture Mechanics*, 72, 1717-1737.
- [19] H. Okada, Endoh, S., & Kikuchi, M. (2005). On fracture analysis using an element overlay technique. *Engineering Fracture Mechanics*, 72, 773-789.